

AD-A047 774

ARMY ELECTRONICS COMMAND FORT MONMOUTH N J  
ELECTRON EMISSION FROM A THIN FILM IV - VI COMPOUND SEMICONDUCT--ETC(U)  
SEP 77 B SMITH, H WEINSTOCK

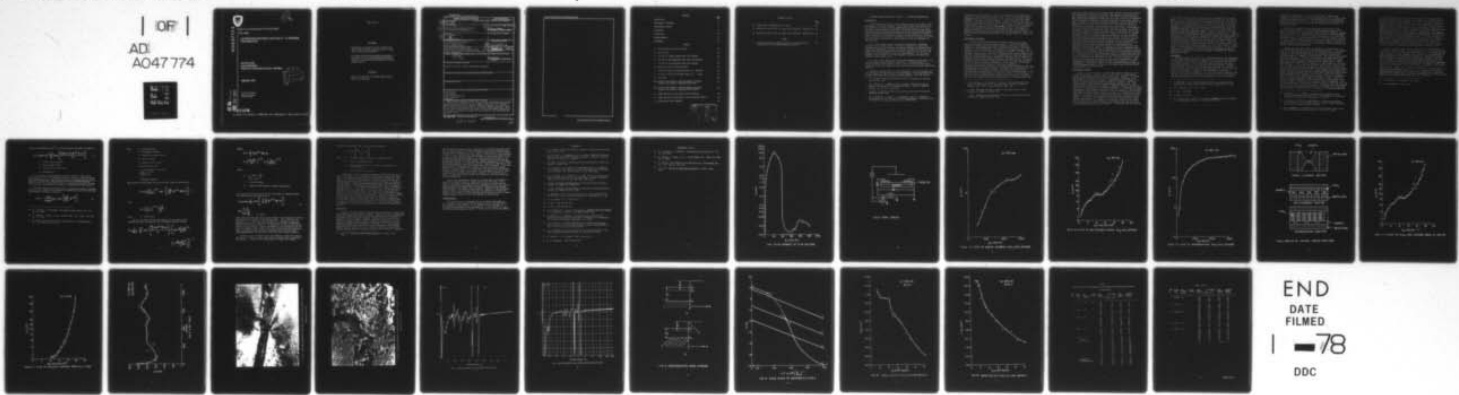
UNCLASSIFIED

ECOM-4534

F/G 20/12

NL

| OF |  
AD:  
A047 774



END  
DATE  
FILED  
1 - 78  
DDC



D  
K

AD A 047774

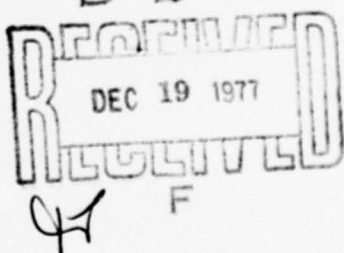
Research and Development Technical Report

ECOM - 4534

ELECTRON EMISSION FROM A THIN FILM IV - VI COMPOUND  
SEMICONDUCTOR

Bernard Smith  
Harvey Weinstock  
Electronics Technology & Devices Laboratory

D D C



September 1977

AD No. \_\_\_\_\_  
DDC FILE COPY

DISTRIBUTION STATEMENT

Approved for public release;  
distribution unlimited.

**ECOM**

US ARMY ELECTRONICS COMMAND FORT MONMOUTH, NEW JERSEY 07703

## **NOTICES**

### **Disclaimers**

The findings in this report are not to be construed as an official Department of the Army position, unless so designated by other authorized documents.

The citation of trade names and names of manufacturers in this report is not to be construed as official Government endorsement or approval of commercial products or services referenced herein.

### **Disposition**

Destroy this report when it is no longer needed. Do not return it to the originator.

## UNCLASSIFIED

SECURITY CLASSIFICATION OF THIS PAGE (When Data Entered)

REPORT DOCUMENTATION PAGE		READ INSTRUCTIONS BEFORE COMPLETING FORM
(14) 1. REPORT NUMBER ECOM - 4534	2. GOVT ACCESSION NO.	3. RECIPIENT'S CATALOG NUMBER
4. TITLE (and Subtitle) Electron Emission From A Thin Film IV - VI Compound Semiconductor.		(9) 5. TYPE OF REPORT & PERIOD COVERED Research and Development Technical Report.
7. AUTHOR(s) Bernard Smith Harvey Weinstock		6. PERFORMING ORG. REPORT NUMBER
8. CONTRACT OR GRANT NUMBER(s)		
9. PERFORMING ORGANIZATION NAME AND ADDRESS US Army Electronics Command (ATTN: DRSEL-TL-BS) Fort Monmouth, NJ 07703		10. PROGRAM ELEMENT, PROJECT, TASK AREA & WORK UNIT NUMBERS (16) 1L7 62705AH94 E3-65
11. CONTROLLING OFFICE NAME AND ADDRESS Beam, Plasma and Display Technical Area US Army Electronics Technology and Devices Lab (ATTN: DRSEL-TL-BS)		(11) 12. REPORT DATE September 1977 (17) E3
13. MONITORING AGENCY NAME & ADDRESS(if different from Controlling Office) (12) 36p.		14. NUMBER OF PAGES 31
16. DISTRIBUTION STATEMENT (of this Report)  Approved for public release; distribution unlimited.		15. SECURITY CLASS. (of this report) Unclassified
17. DISTRIBUTION STATEMENT (of the abstract entered in Block 20, if different from Report)		
18. SUPPLEMENTARY NOTES		
19. KEY WORDS (Continue on reverse side if necessary and identify by block number) semiconductor cold cathodes IV-VI compound emitters primary emission tin-oxide		
20. ABSTRACT (Continue on reverse side if necessary and identify by block number) The emission properties of thin film tin-oxide cold cathodes are reported. Indications of the relative effect of doping concentrations and thickness on emission properties are also included. Empirical analysis of the emission data is made and utilized to indicate the possible emission mechanism. Based on the results obtained during the course of this study, comments are given on this emitter's potential as a practical cold cathode for low and medium power microwave tubes.		

DD FORM 1 JAN 73 EDITION OF 1 NOV 65 IS OBSOLETE

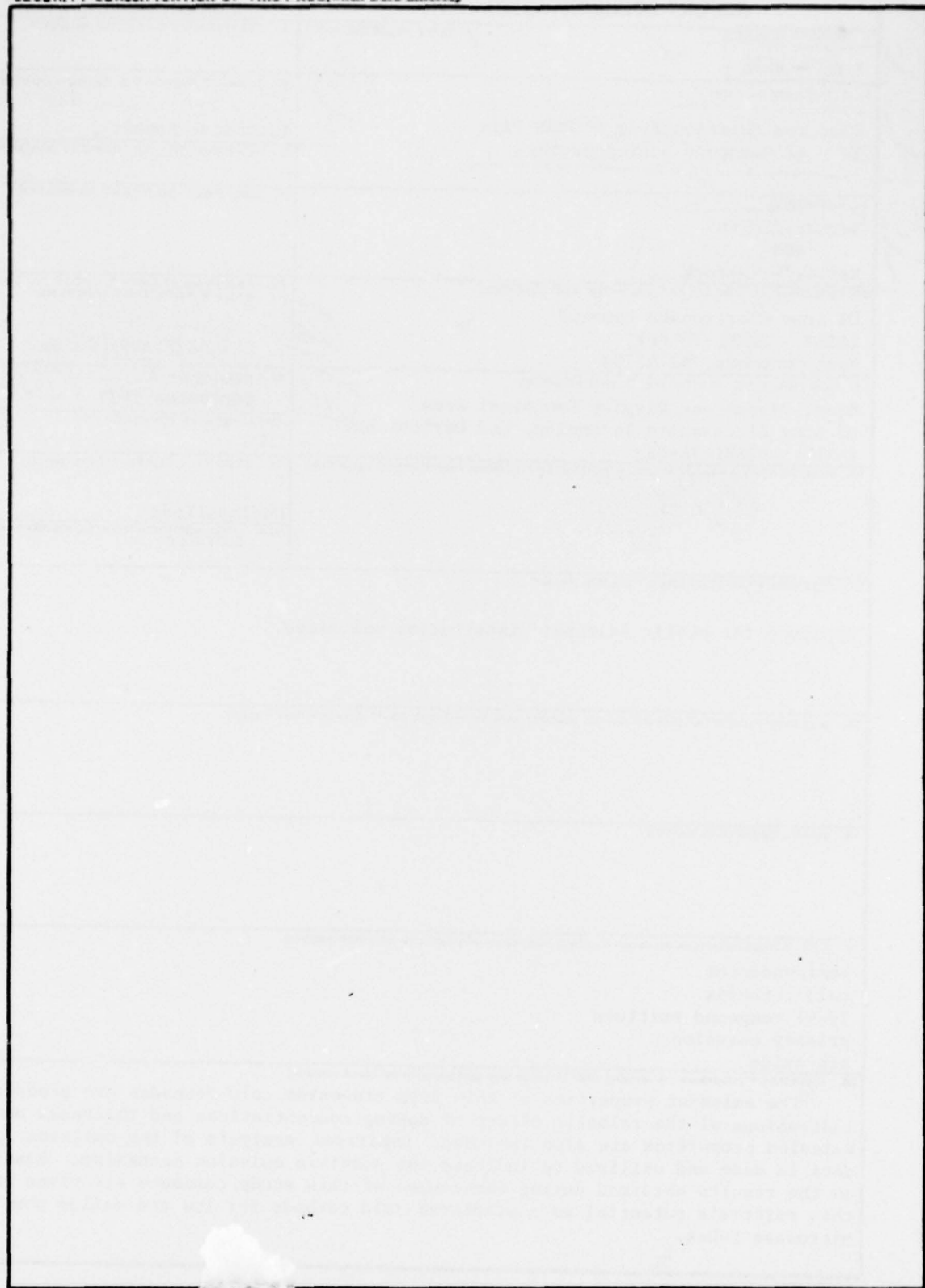
UNCLASSIFIED

SECURITY CLASSIFICATION OF THIS PAGE (When Data Entered)

037620

hb

SECURITY CLASSIFICATION OF THIS PAGE(When Data Entered)



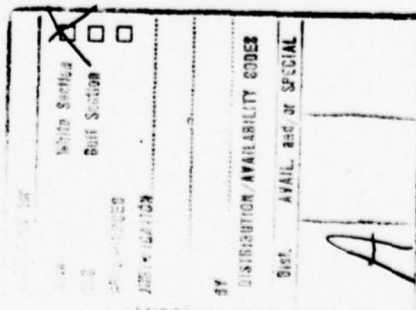
SECURITY CLASSIFICATION OF THIS PAGE(When Data Entered)

## CONTENTS

	<u>Page</u>
INTRODUCTION	1
EXPERIMENTAL PROCEDURE	2
EXPERIMENTAL RESULTS	3
DISCUSSION	4
CONCLUSIONS	10
ACKNOWLEDGMENTS	11
REFERENCES	12

## FIGURES

1. Film Current Versus Film Voltage.	14
2. Test Circuit.	15
3. I-V Plot of Single Element $\text{SnO}_2$ Cold Cathode.	16
4. I-V Plot of Multielement Array $\text{SnO}_2$ Cold Cathode.	17
5. I-V Plot of Interdigitated $\text{SnO}_2$ Cold Cathode.	18
6. Sketch of Various Teated Emitters.	19
7. I-V Plot of $\text{SnO}_2$ Cold Cathode Array, $E_f = 180$ Vdc.	20
8. I-V Plot of $\text{SnO}_2$ Cold Cathode Array, $E_f = 0$ Vdc.	21
9. Life Test.	22
10a. Electron Micrograph of Emitting Region of Single Element $\text{SnO}_2$ Emitter, (Magnification 470X).	23
10b. Electron Micrograph of Emitting Region of Single Element $\text{SnO}_2$ Emitter, (Magnification 1000X).	24
11. Auger Spectrum of $\text{SnO}_2$ Emitter Before Heating.	25
12. Auger Spectrum of $\text{SnO}_2$ Emitter After Heating to $900^\circ\text{C}$ .	26
13. Semiconductor Band Diagram.	27



CONTENTS (Contd.)

	<u>Page</u>
14. Field Plots of Equations 2,3,4 and 5.	28
15. Modified Field Plot of SnO <sub>2</sub> Cold Cathode, (Emitter 1)	29
16. Modified Field Plot of SnO <sub>2</sub> Cold Cathode, (Emitter 2)	30

TABLE

1. Significant Operating Characteristics of a Representative Cross-Section of the Various Emitters Studied.	31
---	----

## ELECTRON EMISSION FROM A THIN FILM IV - VI COMPOUND SEMICONDUCTOR

### INTRODUCTION

Since 1960 there has not been an extensive amount of research in the development of new cold cathodes. Present day military requirements exist for long life, reliable radar and communication systems which are vastly superior to those presently available. The devices needed to meet these requirements, such as low power microwave tubes and solid-state vacuum amplifiers (Electron Beam Semiconductors (EBS)), require emitters which have a unique capability well beyond the present day state-of-the-art. The feasibility of meeting these emitter requirements is directly related to the life and reliability of the electron sources which are the key components of these devices.

Most of the present vacuum tube devices incorporate a thermionic cathode as the electron emitter. Thermionic cathodes have undesirable characteristics such as slow warm-up, unwanted heating of contiguous parts of the tube, unwanted by-products from the hot cathode that coat tube components and lead to premature device failure, sensitivity to failure from vibration, and a broad electron velocity distribution. Use of a cold cathode could alleviate all of these unwanted properties in addition to improving overall device life.

In recent years, research effort has been expended on three basic cold cathode primary emission sources. These are: a) field emitters,<sup>1,2</sup> b) active surface cold cathodes,<sup>3</sup> and c) a new cold electron source (tin oxide)<sup>4</sup> which does not require an active metal coating to achieve appreciable emission.

The major limiting factor to the utilization of the field emitter as a cold cathode source has been the vacuum requirement, and the extremely high voltages which have been required to obtain emission. The high voltage

1. C. A. Spindt, "Novel Field Emission Devices," Conference on Electron Devices, Mar 1973.
2. R. F. Feeney, A. J. Chapman, and B.A. Keener, "High Field Electron Emission From Oxide-Metal Composite Materials," Journal of Applied Physics, Vol. 46, No. 4, Apr 1975.
3. H. Shade, H. Kressel, "Optoelectronic Electron Emitter," Contract No. DAAB07-71-C-0059, 1971.
4. M. I. Elinson, A. G. Zhdan, G. A. Kudintseva, and M. E. Chugunova, "The Emission of Hot Electrons and the Field Emission of Electrons from Tin Oxide," Rad. Eng Elec Phys. 10, pp. 1290, 1965.

requirements of these emitters present some problems in beam modulation control required for amplifier applications. Active surface cold cathodes (**cesiated** surfaces) have never been able to demonstrate prolonged stable operation in practical tube environments. Earlier research on tin oxide ( $\text{SnO}_2$ ) cold cathodes by Elinson, and by Soellner<sup>5</sup> et al, indicated that the problems which limit the application of cold cathodes reported in references 1 and 2 were not present in tin oxide **emitter**. Because of the attractive emission efficiencies reported by Elinson and Soellner, ECOM funded two limited programs<sup>6,7</sup> to do a feasibility study on  $\text{SnO}_2$  cold cathodes for application in microwave devices which were under development at ECOM. This report discusses the work done on  $\text{SnO}_2$  cold cathodes which was carried out at ECOM.

#### EXPERIMENTAL PROCEDURE

The cold cathode structures were tested and fabricated for ECOM under the contracts cited in references 6 and 7. Some of the emitters tested were fabricated by vapor phase deposition on a quartz substrate as follows: a liquid suspension of tin chloride solution  $\text{SnCl}_4 \cdot 5\text{H}_2\text{O}$  was deposited on a hot substrate by utilization of a nitrogen carrier<sup>2</sup> gas to a thickness of 0.1 to  $1.5\mu$  and film resistance from  $10^2$  to  $10^3$  ohms. The resistances obtained were a function of doping (in most cases antimony) and the film cross-sectional area. After deposition, the films were supplied to ECOM for metalizing and emission analysis to determine their potential for becoming a viable cold cathode for microwave tube applications. During the program cited in reference 7, deposition of these films was made by hydrolysis of tin chloride (doped and undoped) on a hot substrate. The devices which were fabricated consisted of single, multielement, and interdigitated emitters fabricated on a planar quartz substrate. The emitters tested during the program were mostly fabricated photolithographically. The coverage region of the  $\text{SnO}_2$  film, where the emitter was formed during activation, was approximately  $3 \times 9$  mils for a single element emitter. A few were fabricated by handscribing the film with a stylus to pre-determine where the emission region would be formed during activation. Activation of the  $\text{SnO}_2$  cold cathode entailed the application of a dc voltage across the

- 
5. A. M. Soellner, J. F. Sprouse, T. A. Raju, "Electron Emission from Region of High Resistance in Tin Oxide Films," Journal of Applied Physics, Vol. 39, No. 3, pp. 1911-1913, Feb. 1968.
  6. J. Mize, "Research and Fabrication of Solid State Emitter Arrays," Contract No. DAAB07-72-C-0195, 1972.
  7. J. Mize, "Research and Development of Non-Active Surface NEA Emitter," Contract No. DAAB07-75-1295-1, 1975.

film until a sharp decline in the film current occurred. This decline usually was accompanied by the onset of emission. Two methods of activation were used. These were designated as being "slow" and "fast" activation processes. The slow procedure consisted of applying the voltage to the film incrementally until activation was indicated by a sharp reduction in film current and the onset of emission. In the fast activation procedure, voltage was applied incrementally in one minute on-off periods until activation occurred as indicated by the previously mentioned decline in film current. During the fast activation procedure when the film currents were above 10 milliamperes, a problem of contact burnout would occur. This did not happen in the slow activation method which entailed incrementally increasing the film voltage periodically until activation took place. Figure 1 is a plot of a typical activation curve for an emitter that was activated by the slow procedure which was primarily utilized throughout this program. The basic test circuit used for activating and testing the emitters was as shown in Figure 2. After activation, the emitters were allowed to age until the emission stabilized at which time I-V data was recorded. During activation visual observation of the emitter was made and the following phenomena was observed. Just prior to activation a region of scintillating white light appeared in the junction region. It was observed that the appearance and intensity of this light was pressure dependent, and after activation occurred the intensity of the light in the junction region was significantly reduced. It is believed that this luminescence was either (1) recombination phenomena, or (2) an ionization of gases generated by extreme localized heating in the junction regions or some combination of both. During activation the magnitude of the film current was usually in the order of milliamperes. After activation the film current ranged from tens of microamperes to several milliamperes. The emission current for each individual emission region was in the microampered range. The area of the single element emitting region was estimated to be  $60 \times 10^{-6} \text{ cm}^2$ .

#### EXPERIMENTAL RESULTS

Figure 3 is an I-V plot of a single element emitter taken at a film voltage of 270 volts. Figures 4 and 5 are I-V plots of a multielement emitter and an interdigitated structure respectively. Figure 6 is a sketch which gives a visual picture of the basic difference in geometry of the emitters cited in Figures 3 through 5. Examining Figures 3 through 5, it can be seen that the emitters have a tendency to saturate as one would normally expect, then increase towards a second saturation level. This second saturation level was not reached in Figures 3 through 5 because I-V data was not continued until the emission saturated. If increases in applied voltage had been continued the emission would have reached the second saturation plateau. This could be indicative of the fact that the total emission from these cathodes is derived from two sources, i.e., thermionic and field emission. This aspect will be discussed in more detail in the next section. Figure 7 is a plot of a multielement emitter which also exhibits the same emission characteristics. Figure 8 is a plot of this same emitter taken at zero film voltage. Upon comparison of Figures 7 and 8, it is observed that the emission in Figure 8 starts at approximately the same point the second emission plateau occurs in Figure 7. This aspect was not observed

in all emitter tests to date as pointed out by Hanasaka et al, in their paper. It is not clear at this point why this phenomena did not occur in all cases or if it is strictly a field dependent occurrence. But part of the reason this was not observed on all emitters may be due to the wide variation in fabrication parameters which was used throughout this study. Hanasaka et al, intimated <sup>8</sup> that the source of this emission may be due to secondary emissions. This will be reviewed in the following section in addition to the field dependence aspect. Figure 9 is a plot of the life test characteristic of what was considered the best emitters (i.e., those doped at  $10^{17}$  to  $10^{18}$  atoms/cm<sup>3</sup>, and a thickness range of  $0.05\mu$  to  $0.10\mu$ ). The fluctuation in emission level as indicated in Figure 9 are quite severe initially, and have a tendency to become more stable during operation. It is believed that the initial severe fluctuations are surface related and as the surface ages in these, fluctuation becomes less severe. Table 1 is a list of significant operating characteristics of a representative cross-section of the various emitters studied. As can be seen, there is a wide range of currents which were achieved from these emitters. In most cases, this could be attributed to the differences in configurations of the emitter types, and the variation in the amount of antimony (Sb) doping of the emitter studied.

#### DISCUSSION

The objective of this study was to investigate the emission properties of SnO<sub>2</sub> cold cathodes in order to understand its operation, and determine its feasibility as a viable cold cathode. In the research that has been done on this emitter to date, several preliminary theories have been generated empirically as to its possible emission mechanism. Elinson<sup>9</sup> et al, believed it may be that the conduction mechanism is the result of field emission between discrete isolated semiconductor sites which is the source of the emission. Mize<sup>10,11</sup>, has developed a curvilinear junction theory which he believes to be the basis for the emission from the SnO<sub>2</sub> cold cathode. More recently Spicer and Powell<sup>12</sup> have proposed a tentative emission model that is field dependent as well as thickness

- 
8. T. Hanasaka, et al, "Electron Emission from Vacuum Evaporated Tin-Oxide Films," Japan Journal Applied Physics, Supplement 2, 1, 1974.
  9. M. I. Elinson, et al - ibid - (#4)
  10. J. Mize - Ibid (#6)
  11. J. Mize - Ibid (#7)
  12. R. A. Powell, W. F. Spicer, "Tin-Oxide and **Related** Oxides with Regard to Cold Cathodes," Contract No. DAAH04-74-0022, 1974.

dependent for achievement of a viable cold cathode. Hartwell and Fonstad<sup>13</sup> intimated that the emission mechanism could be by either field emission, or thermionic emission. Raju and Harrell<sup>14</sup> have reported that they achieved sustained secondary electron emission from SnO<sub>2</sub> films which lead them to suspect that the emission mechanism may be attributed to secondary emission.

Based on the emission data and experimental observation of the emitter tested at ECOM, it is believed that the emission mechanism for SnO<sub>2</sub> cold cathodes is neither strictly field emission, thermionic emission nor secondary emission. Mendenhall<sup>15</sup> reported that the maximum secondary emission ratio ( $\delta$ ) for SnO<sub>2</sub> on a glass substrate was 1.11 at 600 volts of primary energy. He also stated that the  $\delta$  was only slightly above one for primary electrons above 300 volts and less than 1600 volts of energy. For this reason it is believed that the secondary emission contribution is minimal and we will disregard it in our discussion of what we believe may be the possible emission mechanism.

Figures 10a and b are electron micrographs of activated SnO<sub>2</sub> cold cathodes at magnifications of 470X and 1000X respectively. It is observed that in each of these emitters there is an irregular channel across the film that is the emission region which was determined by viewing the cathode emission on a phosphor coated collector. The width of this channel is on the order of 1 to 3 microns. Resistance probe measurements have definitely established that the high resistance region which is formed after activation is completely inclosed in the channel region. These measurements have shown that the resistance in this channel can vary from  $10^3$  -  $10^7$  ohms. If one calculates the power density which would be dissipated in this narrow region it is apparent that the source of some of the visible light which has been observed by investigators to date would indeed be internal heating in the junction or channel region which converts the SnO<sub>2</sub> to an Sn<sub>x</sub>O<sub>y</sub> compound which has a much lower conductivity than the SnO<sub>2</sub> doped compound prior to heating. In an effort to study this transition on a microscopic scale, Auger analysis was made of a large area sample to study the effects of heating on SnO<sub>2</sub> cold cathode surface. Figures 11 and 12 are Auger spectrums of these emitters prior to heating and after heating to 900°C. Comparison of the relative change in magnitude of tin to oxygen peaks prior to heating, and after heating it is seen that they are relatively constant at least on the surface. The sample which was analyzed was supposed to have been doped with Sb but as indicated in the spectrum shown in Figures 11 and 12 there is no Sb peak. It is believed that this

- 
13. M. Hartwell, C. G. Fonstad, "Strong Electronic Emission from Patterned Tin-Indium Oxide Thin Films," Proceedings of International Electron Devices Meeting, Washington, D.C., 1975.
  14. T. A. Raju, B.J. Harrell, "Manifestation of Substained Secondary Electron Emission from Tin-Oxide Films," Journal of Applied Physics, Vol. 40, No. 10, pp. 4213-4214, Sep 1964.
  15. H. E. Mendenhall, "Secondary Emission from Conducting Films of Tin-Oxide," American Physical Society, Vol. 532, No. 62, 1949.

is because the quantity of Sb in the emitter was less than that which could be detected by Auger analysis. The significant information showed the effect heating in the vacuum had on the  $\text{SnO}_2$  cold cathode surface. Indications were that at the maximum obtainable temperature of  $900^\circ\text{C}$  the change in relative composition was small. This would indicate that this temperature was not high enough to cause the composition changes which took place as a result of internal heating of  $\text{SnO}_2$  film by passing current through the junction in a vacuum. Based on the intensity of the glow which occurred just prior to activation, it appeared that the temperature in the junction in a necked down emitter was much higher. Because of the relatively small areas of the junction region ( $2\mu \times 100\mu$ ) accurate measurement of the channel temperature was very difficult by conventional means. After heating, it was found that the resistance of the film examined in the Auger system had increased, but not the three to six orders of magnitude that had been observed when activating the emitters by passing current through the necked down region of the  $\text{SnO}_2$  film.

Figures 3 through 5 are typical curves of the I-V characteristics of the emitters studied to date. It is observed that the curve does not give a good fit to any of the aforementioned theories. It is believed that the double maximum is voltage dependent and is the result of a combination of emission mechanism. As intimated by Hartwell and Fonstad<sup>16</sup> we believe that the primary mechanism for this cathode based on empirical analysis is a combination of field emission, and thermionic emission with a very small contribution generated by secondaries. For the sake of our discussion, and since we believe the secondary contribution is minimal<sup>17</sup> we will disregard this contribution to the total emission at pressures of  $10^{-5}$  Pascal (Pa) or better. Figure 13 is a model of the  $\text{SnO}_2$  cold cathode which is a wide-band gap semiconductor where  $E_g = 3.2$  eV. Figure 13a is the band diagram before application of an electric field and Figure 13b shows the surface barrier bending which occurs after application of an electric field high enough to initiate field emission (i.e.,  $> 10^7$  V/cm).

---

16. M. Hartwell, C. G. Fonstad - Ibid (#13)

17. H. E. Mendenhall - Ibid (#15)

The Fowler-Nordheim equation<sup>18</sup> for field emission from metals is given as:

$$J = 1.54 \times 10^{-6} \frac{E^2}{\phi} \exp - \left[ \frac{6.83 \times 10^7 \phi^{3/2} F(Y)}{E} \right] \quad (1)$$

J = current density ( $\text{A}/\text{cm}^2$ )

E = field strength ( $\text{V}/\text{cm}$ )

$\phi$  = surface work function (eV)

T = temperature  $^{\circ}\text{K}$

$F(y)$  is given as a dimensionless elliptic function. Fowler found that at fields of  $10^7 \text{ V/cm}$ , emission occurs as a result of electron tunnelling through the barrier. While Equation 1 is quite satisfactory for metals, emission from  $\text{SnO}_2$  cold cathodes do not adhere to the Fowler-Nordheim theory because of (1) field penetration, (2) internal heating which occurs as a result of  $I^2R$  dissipation, (3)  $\text{SnO}_2$  is a semiconductor not a metal.<sup>19</sup>

Straton<sup>20</sup> reported that emission from a semiconductor without a surface barrier for the condition that emission by tunnelling is much more important than thermionic emission is given by:

$$J \approx ne \frac{2kT}{(2m\phi)^{1/2}} \exp - \left[ \frac{4\bar{k}}{3E} \phi^{3/2} \right]. \quad (2)$$

- 
18. R. H. Fowler, L. N. Nordheim "Proceedings Royal Society, Vol. 173, pp. 119, 1928.
  19. K. Ishiguri, T. Sasaki, et al., Journal Phys. Soc., Japan, Vol. 296, pp. 13, 1958.
  20. R. Straton, "Field Emission from Semiconductors," Proceedings Phys. Soc., Vol. B68, pp. 746, 1955.

where             $e$  = electron charge  
 $k$  = Boltzmann's constant  
 $T$  = temperature degrees Kelvin  
 $m$  = mass of charge  
 $E$  = applied field in V/cm  
 $\phi$  = work function (eV)  
 $n$  = concentration of electrons  
 $\bar{K} = \left( \frac{8m\pi^2}{h^2} \right)^{1/2}$   
 $h$  = Planck's constant

When Stratton included image forces, the emission equation was given by:

$$J = ne \left( \frac{kT}{2\pi m} \right)^{1/2} \exp - \left[ \frac{4\bar{K}}{3E} \phi^{3/2} \Phi(U) \right] \quad (3)$$

where

$$U = \left( \frac{\epsilon - 1}{\epsilon + 1} \right)^{1/2} \frac{e\sqrt{E}}{\phi}$$

where             $\epsilon$  = permittivity

For the case where we have both image force and surface field penetration states the equation for the emission density becomes:

$$J \simeq \frac{e}{8\pi h} \frac{E^2}{\phi} \exp - \left( \frac{\frac{4}{3}\bar{K}\phi^{3/2}\Phi(U)}{E} \right) \left[ \exp \frac{2\bar{K}v\phi^{1/2}}{E^{1/5}} - \left( 1 + \frac{2\bar{K}v\phi^{1/2}}{E^{1/5}} \right) \right] \quad (4)$$

where

$$E \ll \frac{2}{3} \bar{K} \phi^{3/2} \Phi(U)$$

$$v = \left( \frac{15\sqrt{\pi}}{16} \right)^{2/5} kT \left( \frac{x_0}{ekT} \right)^{4/5}$$

where

$$x_0 = \left( \frac{ekT}{16\pi N_0 e} \right)^{1/2}$$

e = electron charge

$N_0$  = impurity concentration at thermal equilibrium

The equation derived by Stratton for the case where he considered image force and surface states was given by:

$$J = J_0 \exp \frac{V}{kT} \exp \left[ -\frac{4}{3} \frac{\bar{K}}{E} \phi^{3/2} \Phi(U) \right] \quad (5)$$

$$J_0 = \frac{n E}{\exp \frac{V}{kT}}, \quad V = \text{volts}$$

Using these equations, and taking typical values of the constants he plotted the emission as a function of the applied field. All of the plots for Equations 2, 3, 4, and 5 are shown in Figure 14. Figures 15 and 16 are modified field plots of  $\text{SnO}_2$  cold cathodes tested at ECOM. In comparing Figures 15 and 16 with curve No. 4 in Figure 14, one can see that the two curves are quite similar. This would indicate that the emission from the curves in Figures 15 and 16 seem to obey the curve plotted from Equation 4, which is the equation for temperature dependent field emission from a semiconductor which has both image force and surface states available.

Curves 2 and 3 of Figure 14 are very similar to those for a metal; the factor  $E^2$  in both of these cases, and in the metal case is relatively unimportant. In the case of semiconductors, currents are strongly

temperature dependent<sup>21</sup> due to the factor n, given by:

$$n = N_c \exp \left\{ \frac{(-E_c - E_f)}{kT} \right\}$$

where  $N_c$  = effective density of states in conduction band

$E_c$  = bottom of conduction band

$E_f$  = Fermi energy level and is defined as the density of free electrons

n = concentration of electrons.

In Equations 2 and 3 it should be pointed out that neither curve 2 nor 3 can apply to a real semiconductor since variations in the lower edge of the conduction band near the surface must be considered. When there is a sufficiently high density of surface states, the internal barrier produced will cause a drop in current with respect to Equation 3 for low fields. As the field increases, the barrier is lowered and the current begins to increase much more rapidly until curve 5 in Figure 14 intersects curve 3 at D which corresponds to the complete breakdown of the barrier, i.e.,  $V = \emptyset$ , when  $E_o = 2.5 \times 10^7$  V/cm. For fields higher than  $E_o$ , field penetration will occur which is the case governed by Equation 4 for an applied field  $E > E_o$ . When  $E - E_o$  is sufficiently large we get the region bounded by AB in Figure 14. Stratton has shown a dashed line to suggest the connection between the two regions on Figure 14. In comparing Figure 15 and 16 with curve 5 in Figure 14, similarities in the three curves are evident, especially in the region bounded by C-E in Figure 14. Similarities in Figures 14, 15, and 16 tends to support our contention that the emission mechanism is temperature-enhanced field emission.

#### CONCLUSIONS

A number of cathode samples which have been fabricated by chemical and vapor phase deposition have been studied. During this study several parameters were varied in an effort to determine their effect on the emission characteristics of  $\text{SnO}_2$  cold cathodes. During the initial stages of operation of these cathodes emission stability was very poor. In most cases after several hours of aging, the emission instability initially observed, disappeared or significantly decreased. All of the emitters tested which gave respectable emission, were operated at film voltages ranging from 60 volts to 425 volts. Emitter efficiency as high as 50 percent has been observed, but only for a very short duration. Sustained

21. S. M. Sze, Physics of Semiconductor Devices, S. Wiley & Sons, 1958.

emitter efficiency ranging from 0.1 percent to 15.8 percent has been recorded. As shown in Table 1 the best efficiencies have been exhibited by the emitters which had dopings of  $10^{17}$  to  $10^{18}$  Sb atoms/cm<sup>3</sup> and a film thickness of  $0.05\mu$  to  $0.1\mu$ . These are the best emission values that have been reported to date for vapor deposited SnO<sub>2</sub> with Sb doping. During the course of this program the emission characteristics of these emitters operating in a low voltage bias mode has also been studied. Though success in this area has been minimal to date, it is believed that through optimization of the doping, and volume parameter of the SnO<sub>2</sub> cold cathode, significant reduction in the operating bias voltage below its present value can be achieved. It has been observed that this cathode has a tendency to deactivate while sitting dormant in a good vacuum. In all cases when this has occurred the emitter has been capable of being re-activated. This phenomena is not fully understood, but it is believed to be surface related. If this emitter is to become a viable cold cathode source, this abnormality must be studied and the cause eradicated.

Based on the experimental results on Sb doped SnO<sub>2</sub> cold cathodes to date, it is believed that this cathode may have the potential to be a viable cold cathode, but before this can be achieved, at least several years of research and development must be performed to resolve the complex problems which still remain, before reliable, reproducible low voltage, high efficiency cold cathode can be practical. Because of the substantial amount of effort and resources which must be expended to optimize this emitter, and in view of the more advanced state-of-the-art of other primary emission sources, effort on this cold cathode was discontinued.

#### ACKNOWLEDGMENTS

The authors wish to acknowledge the able technical assistance of Mr. A. Newman in the design of the test devices and for his fabrication, and assembly of these devices; Mr. T. Szwajer for his assistance in building and modifying the test equipment; Mr. E. Daly, and Mr. W. Smith for their technical support; and Mr. G. Taylor for his review and comments.

#### REFERENCES

1. C. A. Spindt, "Novel Field Emission Devices," Conference on Electron Devices, Mar 1973.
2. R. F. Feeney, A. J. Chapman, and B. A. Keener, "High Field Electron Emission Iron Oxide-Metal Composite Materials," Journal of Applied Physics, Vol. 46, No. 4, Apr 1975.
3. H. Shade, H. Kressel, "Optoelectronic Electron Emitter, Contract No. DAAB07-71-C-0059, 1971.
4. M. I. Elinson, A. G. Zhdan, G. A. Kudintseva, and M. E. Chugunova, "The Emission of Hot Electrons and the Field Emission of Electrons from Tin Oxide," Rad. Eng Elec Phys. 10, pp. 1290. 1965.
5. A. M. Soellner, J. F. Sprouse, T. A. Raju, "Electron Emission from Region of High Resistance in Tin Oxide Films," Journal of Applied Physics, Vol. 39, No. 3, pp. 1911-1913, Feb. 1968.
6. J. Mize, "Research and Fabrication of Solid State Emitter Arrays." Contract No. DAAB07-72-C-0195, 1972.
7. J. Mize, "Research and Development of Non-Active Surface NEA Emitter," Contract No. DAAB07-75-1295-1, 1975.
8. T. Hanasaki, et al, "Electron Emission from Vacuum Evaporated Tin-Oxide Films," Japan Journal Applied Physics, Supplement 2, 1, 1974.
9. M. I. Elinson, et al - (See Ref #4).
10. J. Mize - Ibid (See Ref #6).
11. J. Mize - Ibid (See Ref #7).
12. R. A. Powell, W. F. Spicer, "Tin-Oxide and Related Oxide with Regard to Cold Cathodes," Contract No. DAAH04-74-0022, 1974.
13. M. Hartwell, C. G. Fonstad, "Strong Electronic Emission from Patterned Tin-Indium Oxide Thin Films," Proceedings of International Electron Devices Meeting, Washington, D.C., 1975.
14. T. A. Raju, B. J. Harrell, "Manifestation of Substained Secondary Electron Emission from Tin-Oxide Films," Journal of Applied Physics, Vol. 40, No. 10, pp. 4213-4214, Sep 1964.
15. H. E. Mendenhall, "Secondary Emission from Conducting Films of Tin-Oxide," American Physical Society, Vol. 532, No. 62, 1949.
16. M. Hartwell, C. G. Fonstad.- Ibid ( See Ref #13).
17. H. E. Mendenhall - Ibid (See Ref #15).

REFERENCES (Contd.)

18. R. H. Fowler, L. N. Nordheim, "Proceedings Royal Society, Vol. 173, pp. 119, 1928.
19. K. Ishiguri, T. Sasaki, et al., Journal Phys. Soc., Japan, Vol. 296, pp. 13, 1958.
20. R. Stratton, "Field Emission from Semiconductors," Proceedings Phys. Soc., Vol. B68, pp. 746, 1955.
21. S. M. Sze, Physics of Semiconductor Devices, S. Wiley & Sons, 1958.

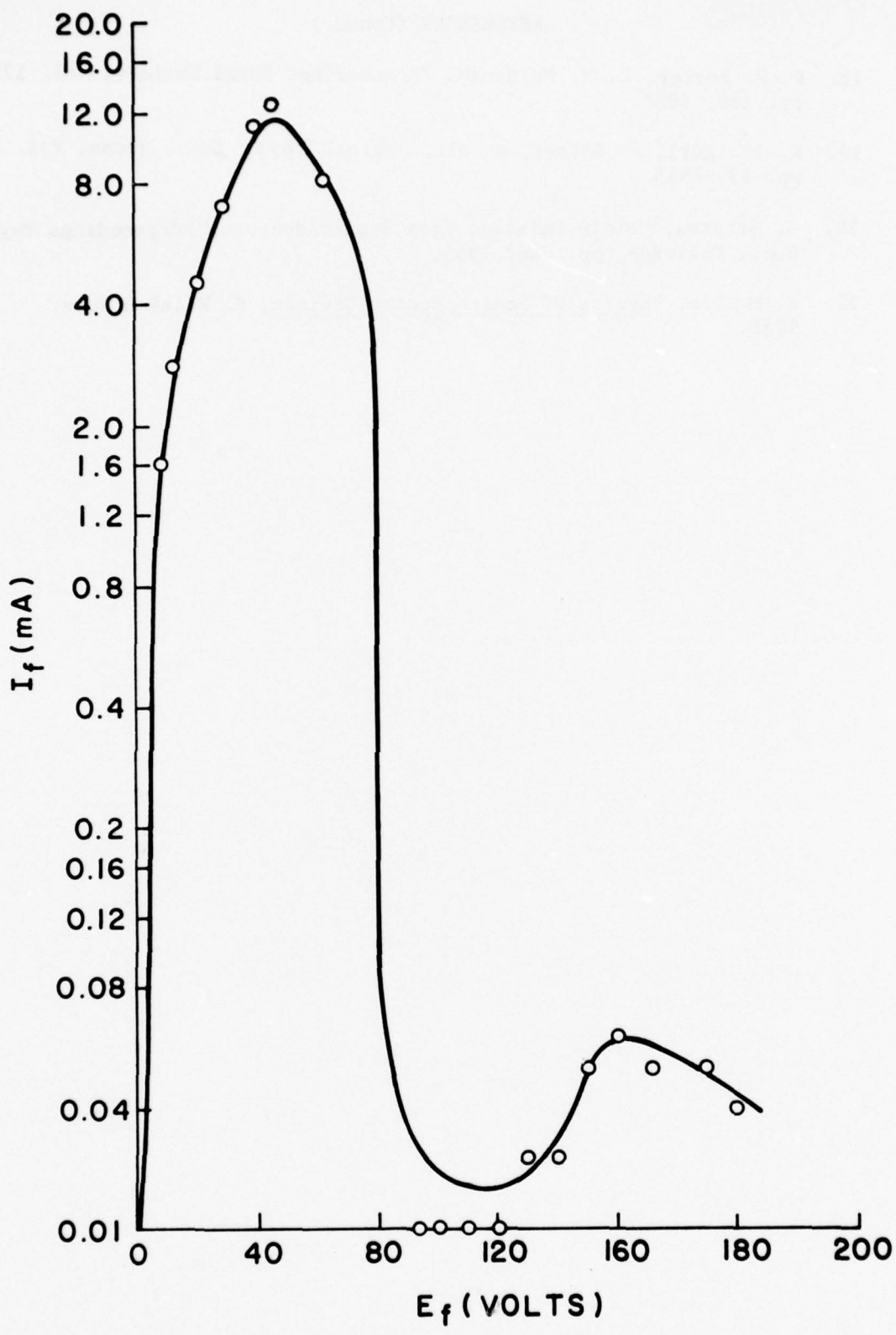


FIG. I FILM CURRENT VS FILM VOLTAGE

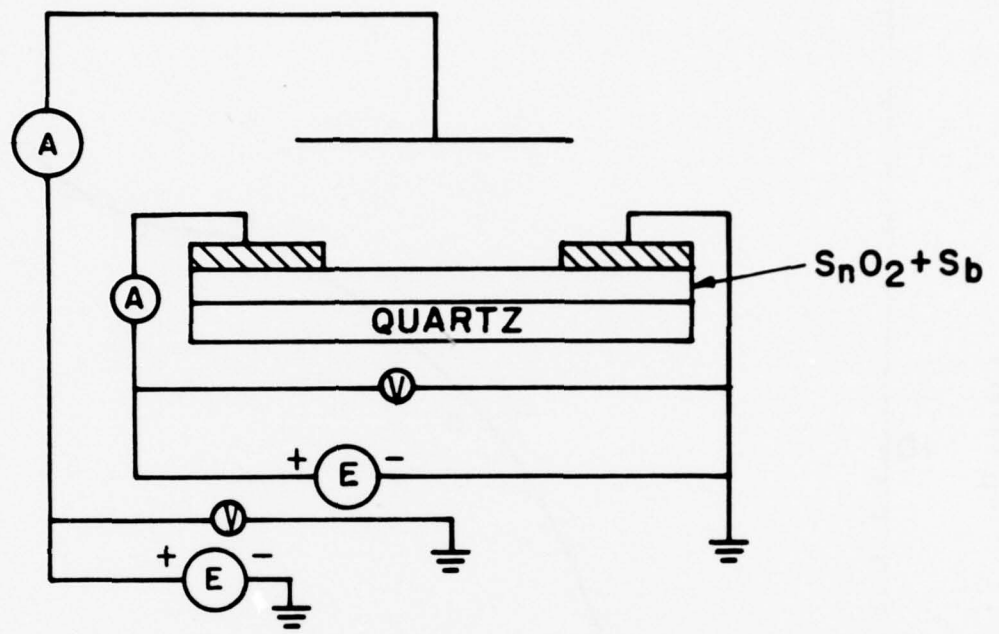


FIG. 2 TEST CIRCUIT

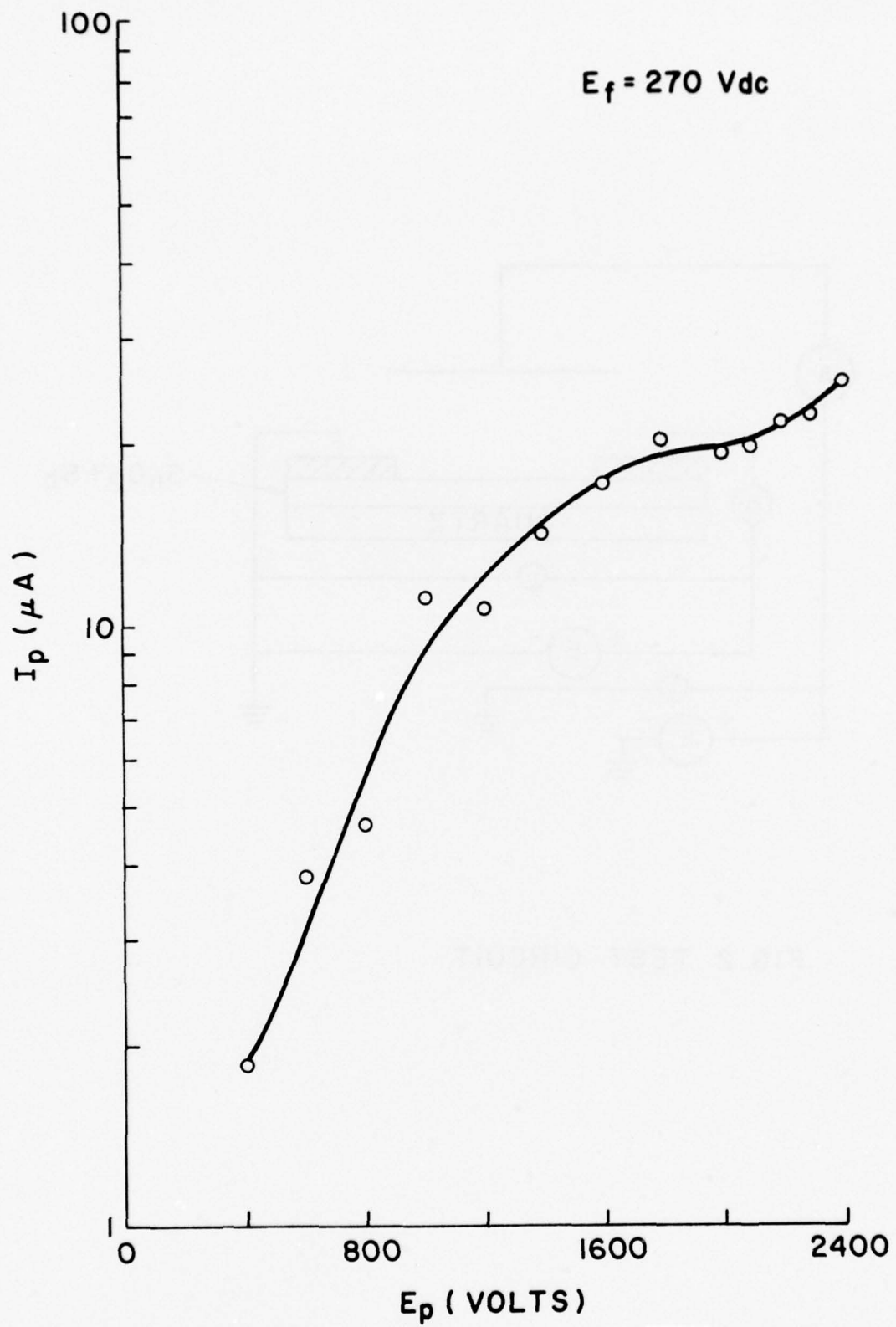


FIG.3 I-V PLOT OF SINGLE ELEMENT  $\text{SnO}_2$  COLD CATHODE

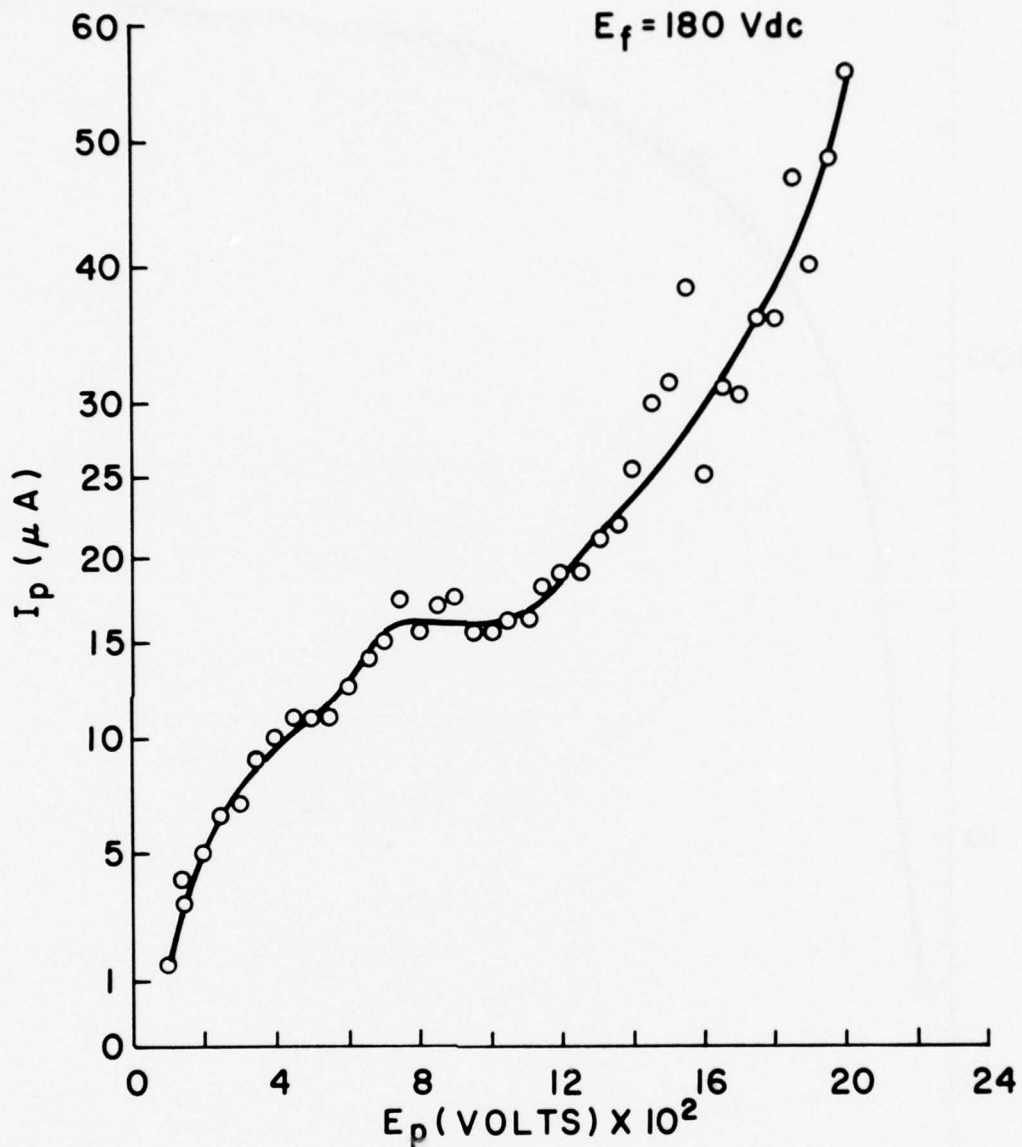


FIG. 4 I-V PLOT OF MULTIELEMENT ARRAY  $\text{SnO}_2$  COLD CATHODE

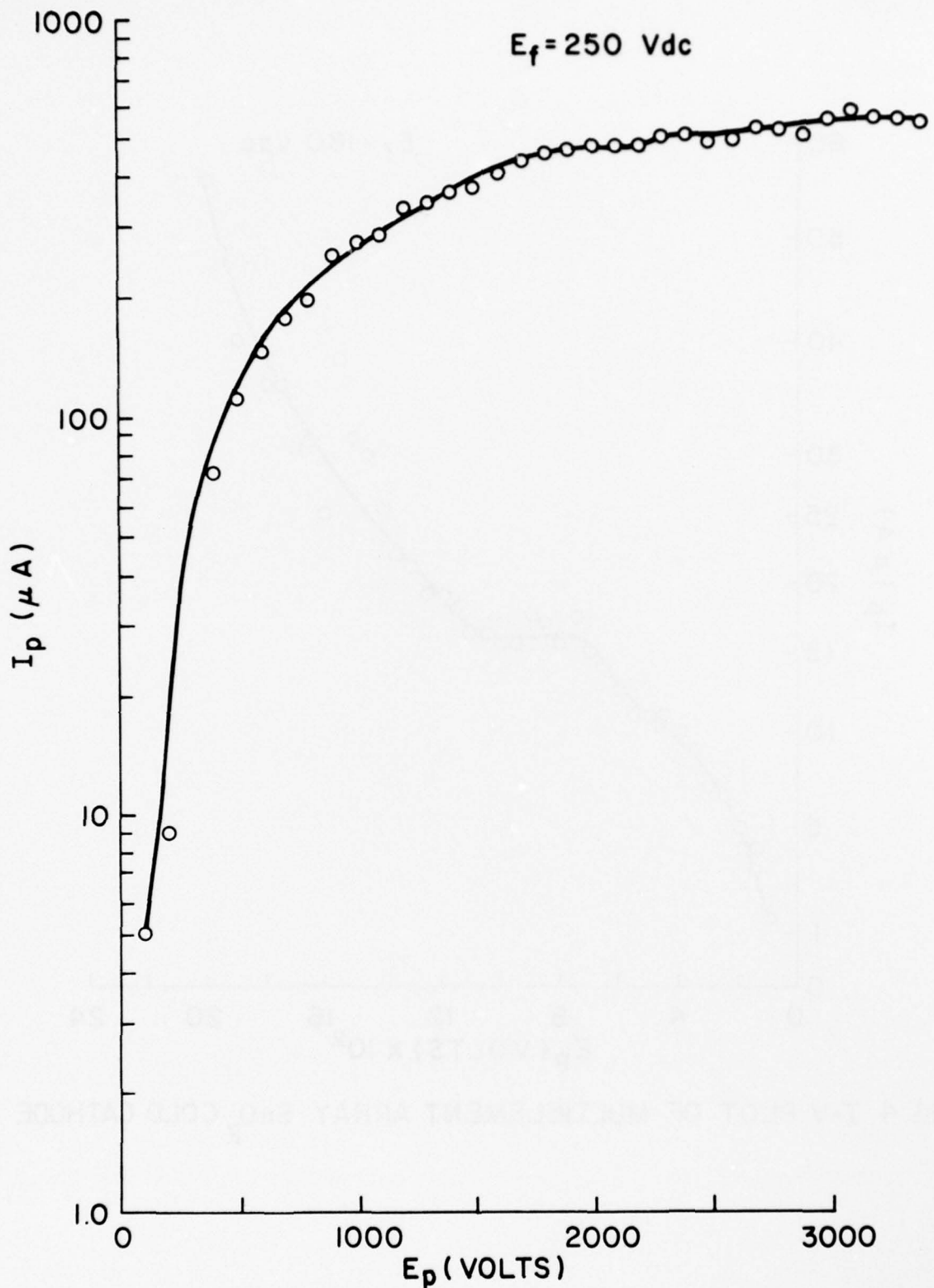
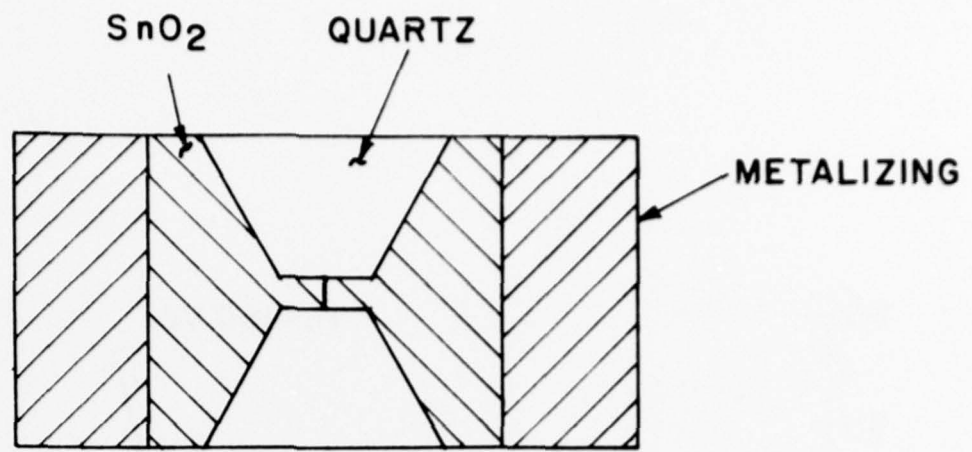
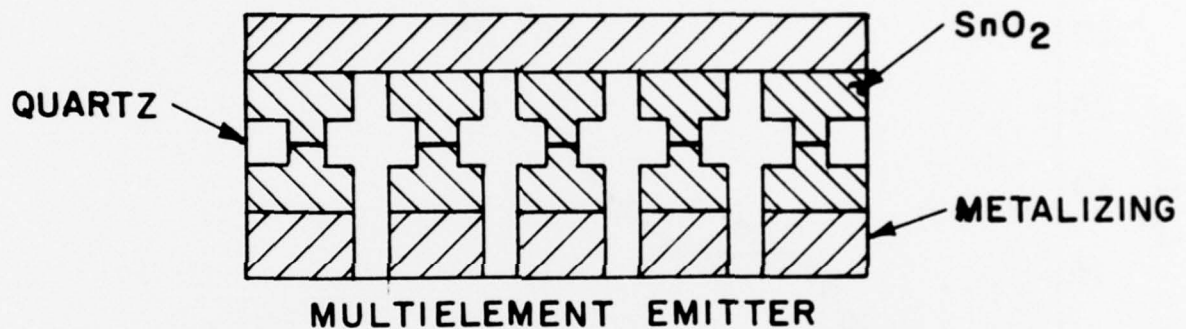


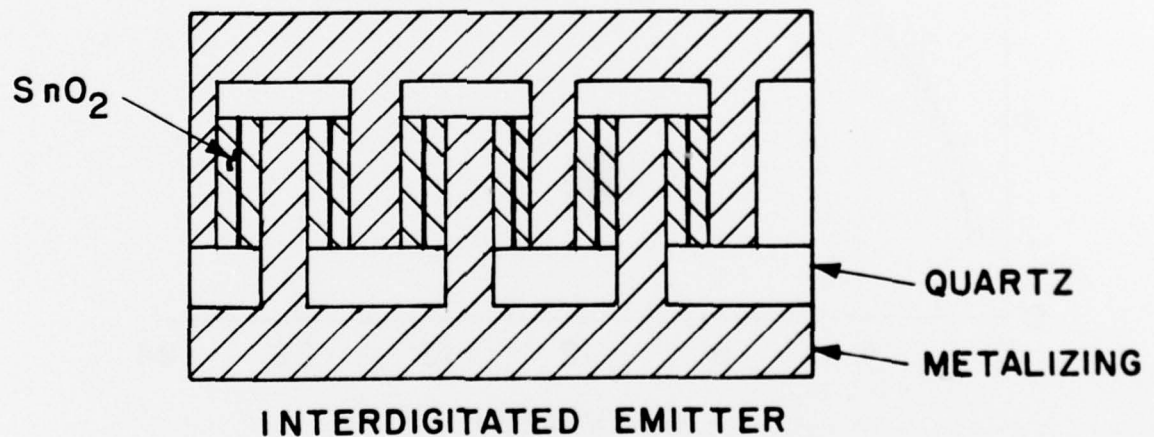
FIG. 5 I-V PLOT OF INTERDIGITATED  $\text{SnO}_2$  COLD CATHODE



SINGLE ELEMENT Emitter



MULTIELEMENT Emitter



INTERDIGITATED Emitter

FIG. 6 SKETCH OF VARIOUS TESTED EMITTERS

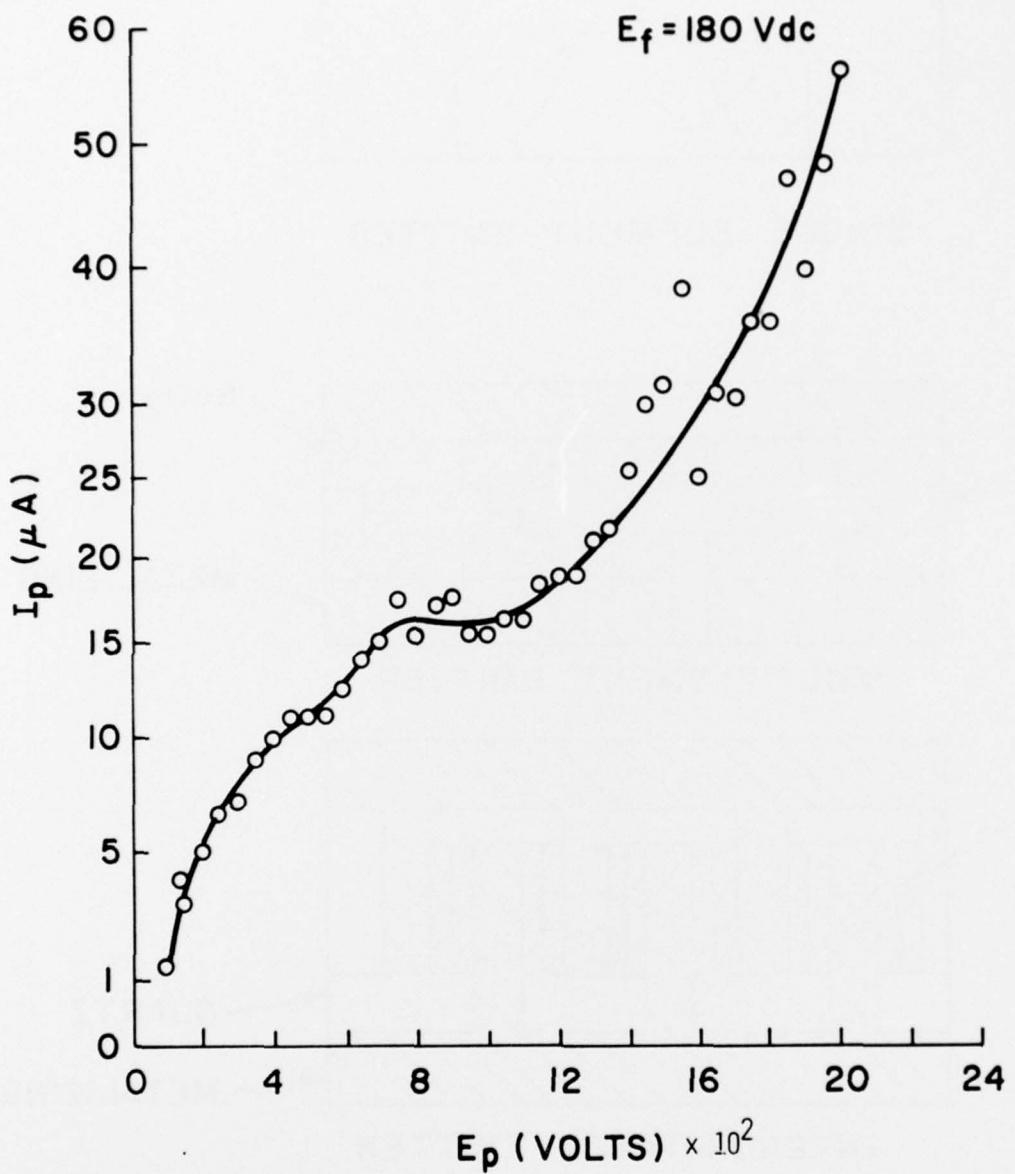


FIG. 7 I-V PLOT OF  $\text{SnO}_2$  COLD CATHODE ARRAY  $E_f = 180 \text{ Vdc}$

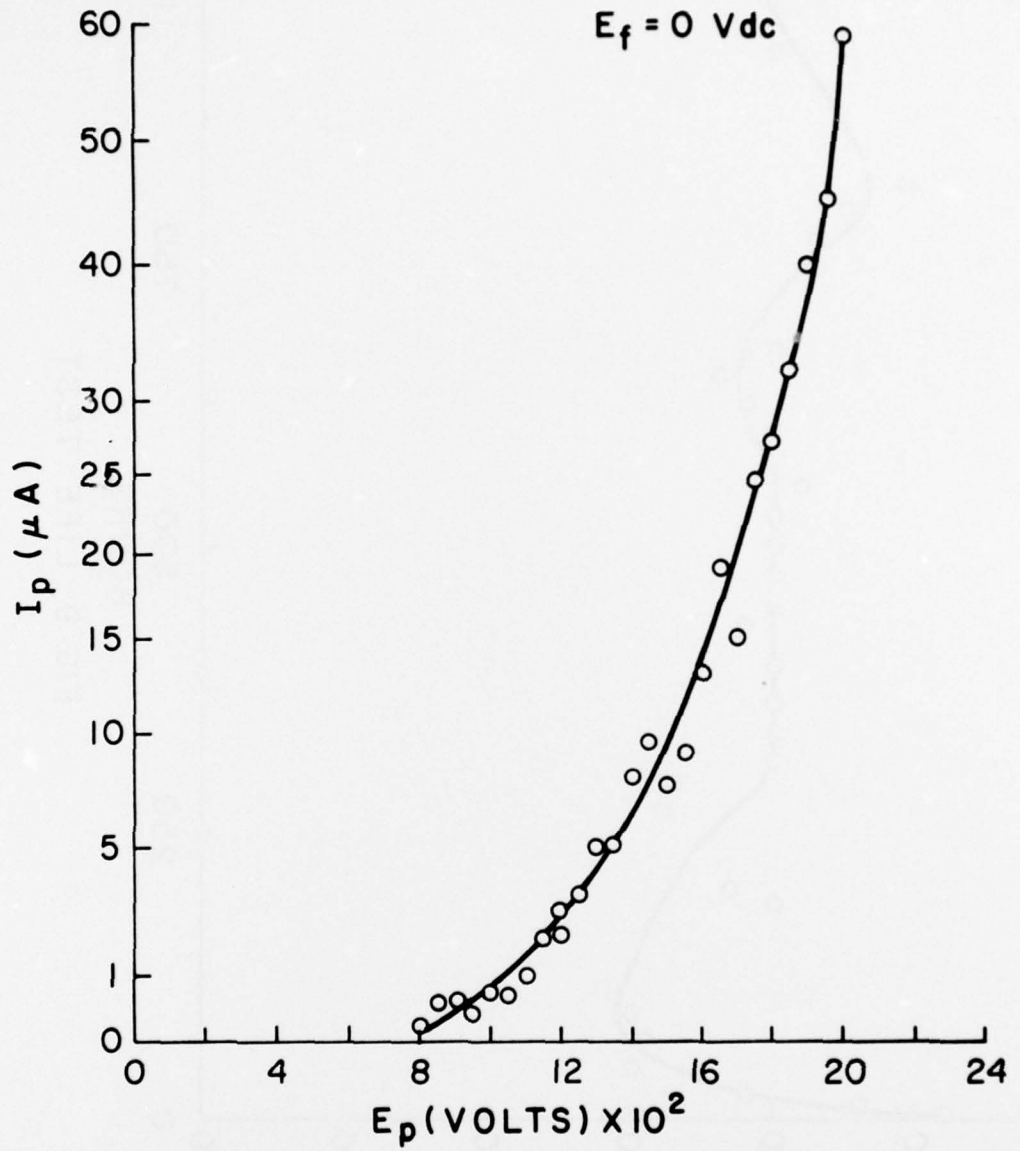


FIG. 8 I-V PLOT OF  $\text{SnO}_2$  COLD CATHODE ARRAY  $E_f = 0 \text{ Vdc}$

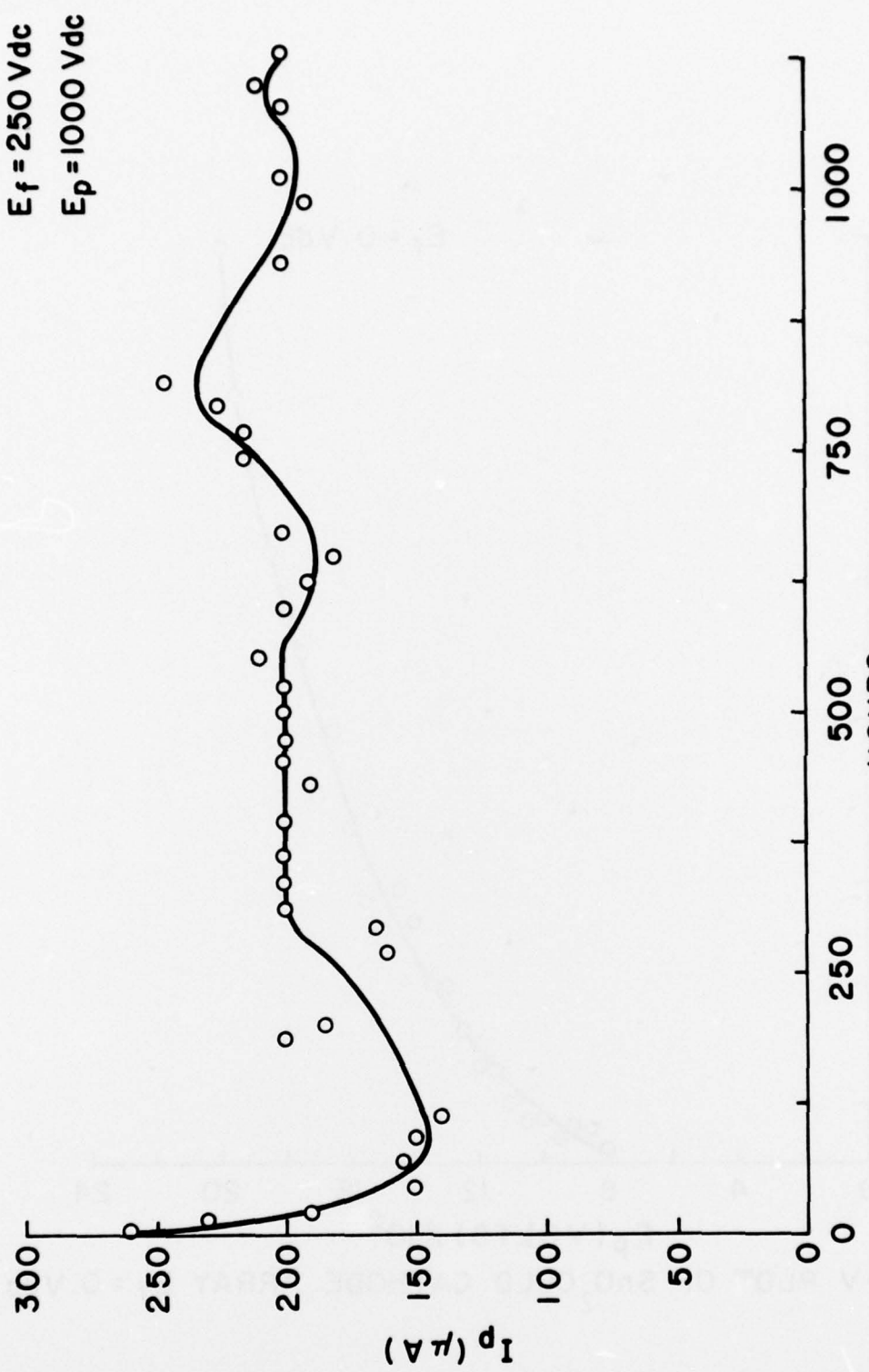


FIG. 9 LIFE TEST



FIG 10a ELECTRON MICROGRAPH OF EMITTING REGION OF SINGLE ELEMENT  $\text{SnO}_2$  Emitter.  
(MAGNIFICATION 470X)



FIG 10b ELECTRON MICROGRAPH OF EMITTING REGION OF SINGLE ELEMENT SnO<sub>2</sub> Emitter .  
(MAGNIFICATION 1000X)

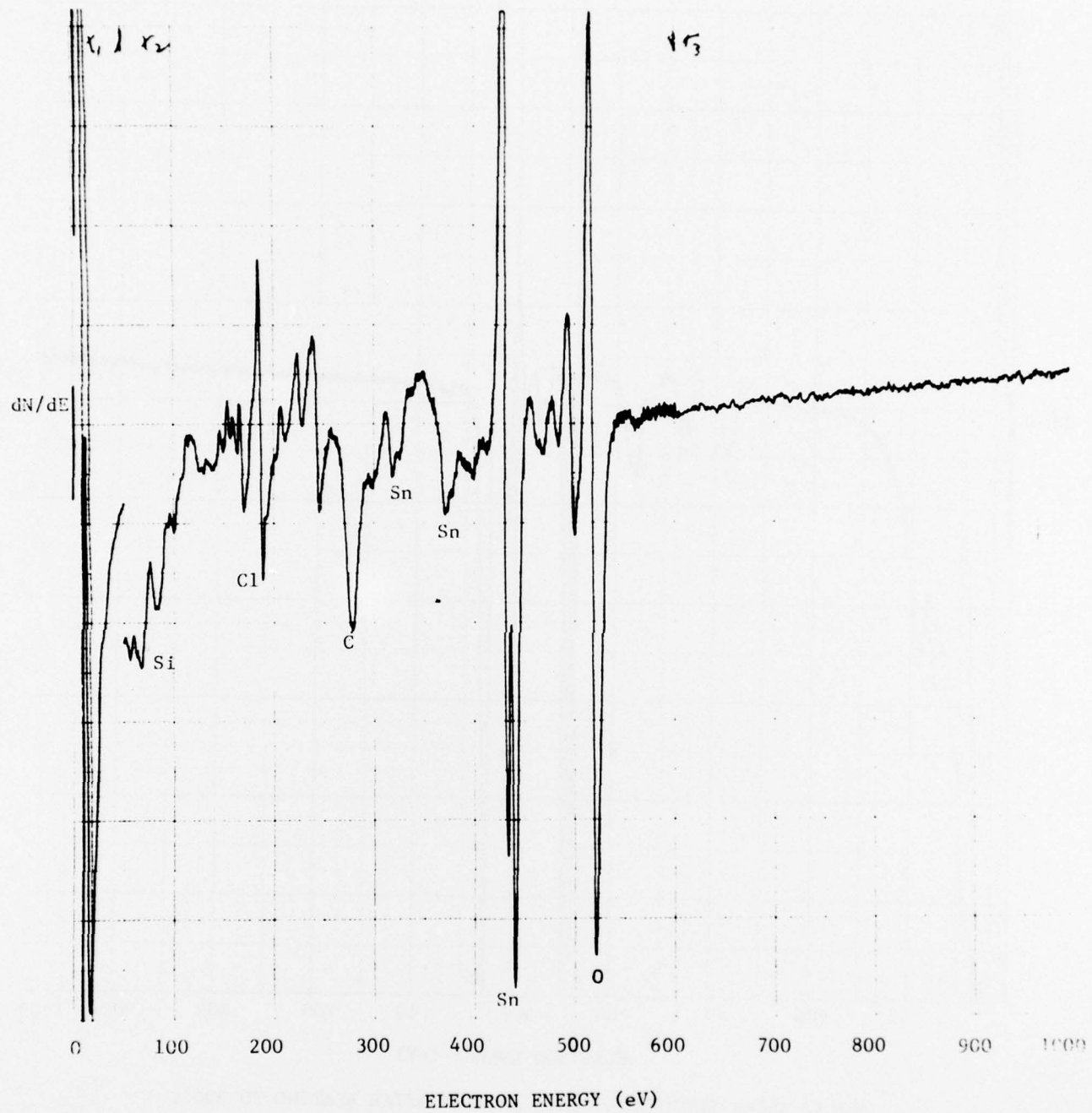


FIG 11 AUGER SPECTRUM OF  $\text{SnO}_2$  Emitter BEFORE HEATING

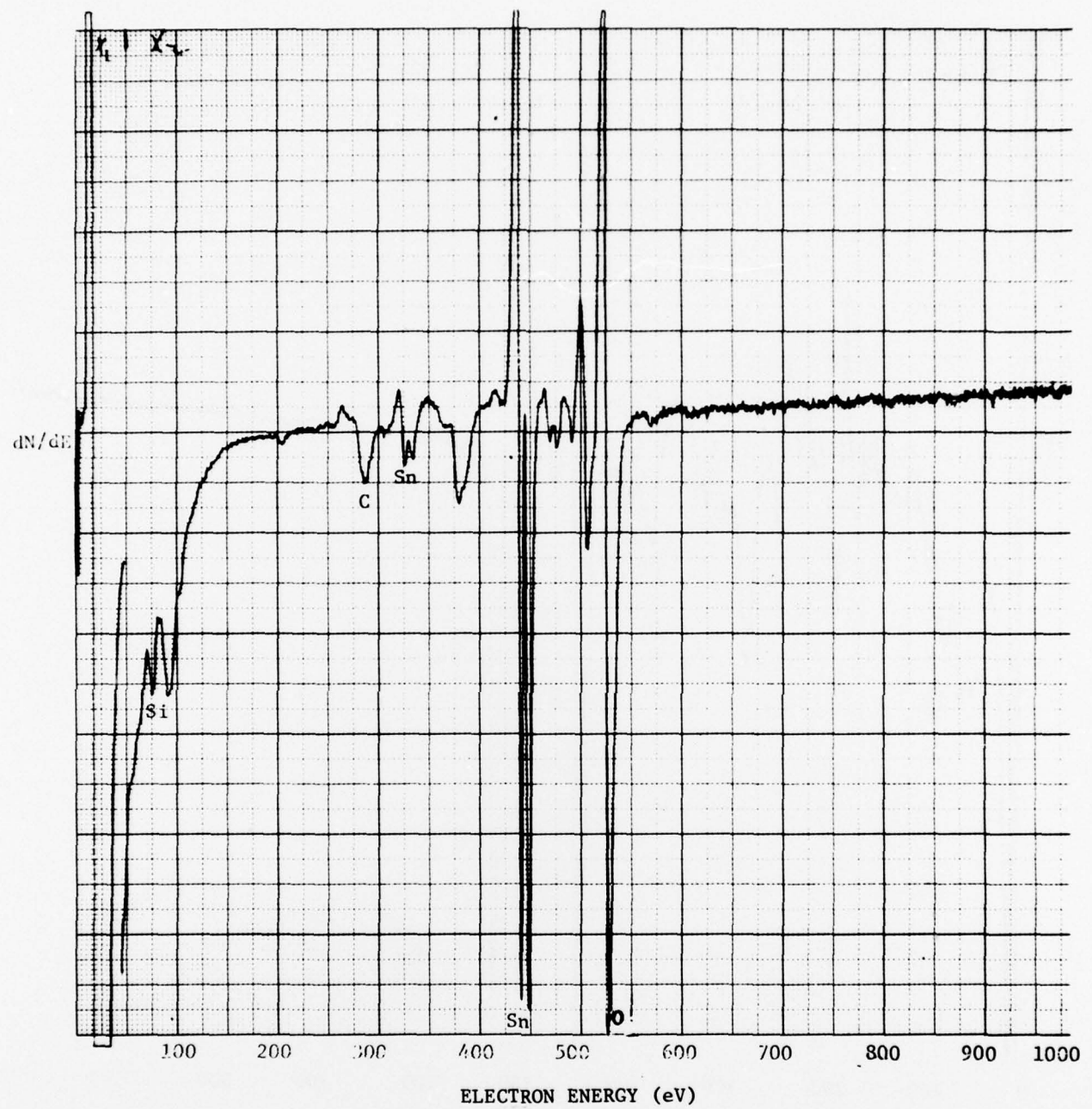
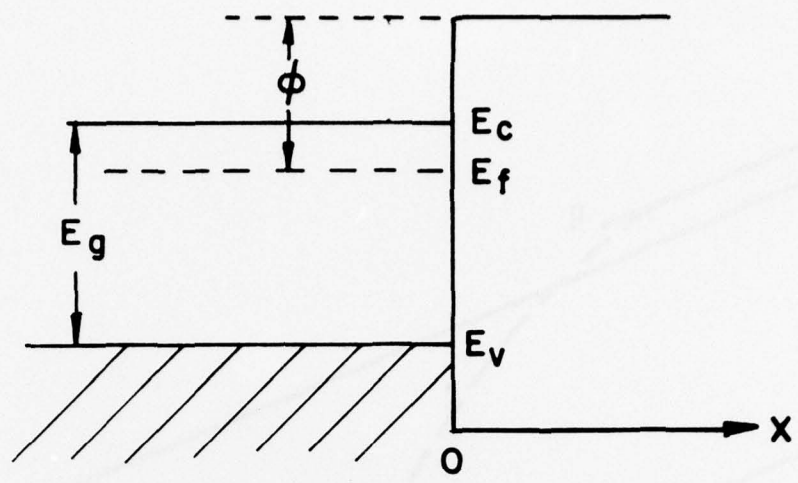
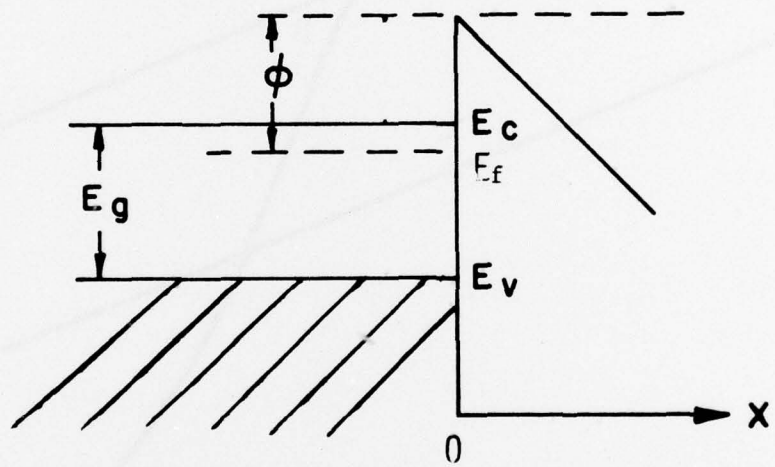


FIG. 12 AUGER SPECTRUM OF  $\text{SnO}_2$  Emitter AFTER HEATING TO 900°C



a



b

**FIG. 13 SEMICONDUCTOR BAND DIAGRAM**

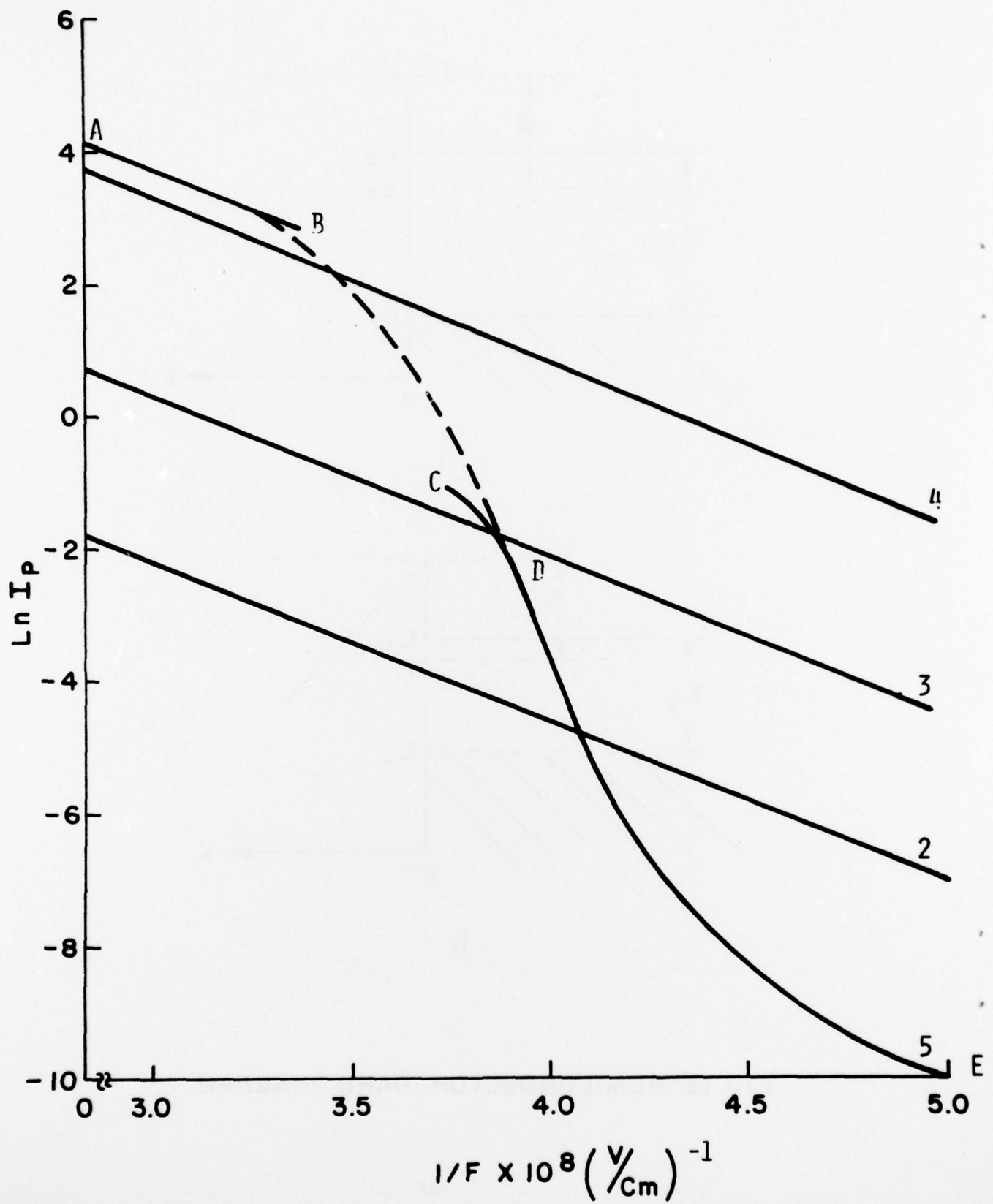


FIG. 14 FIELD PLOTS OF EQUATIONS 2, 3, 4 & 5

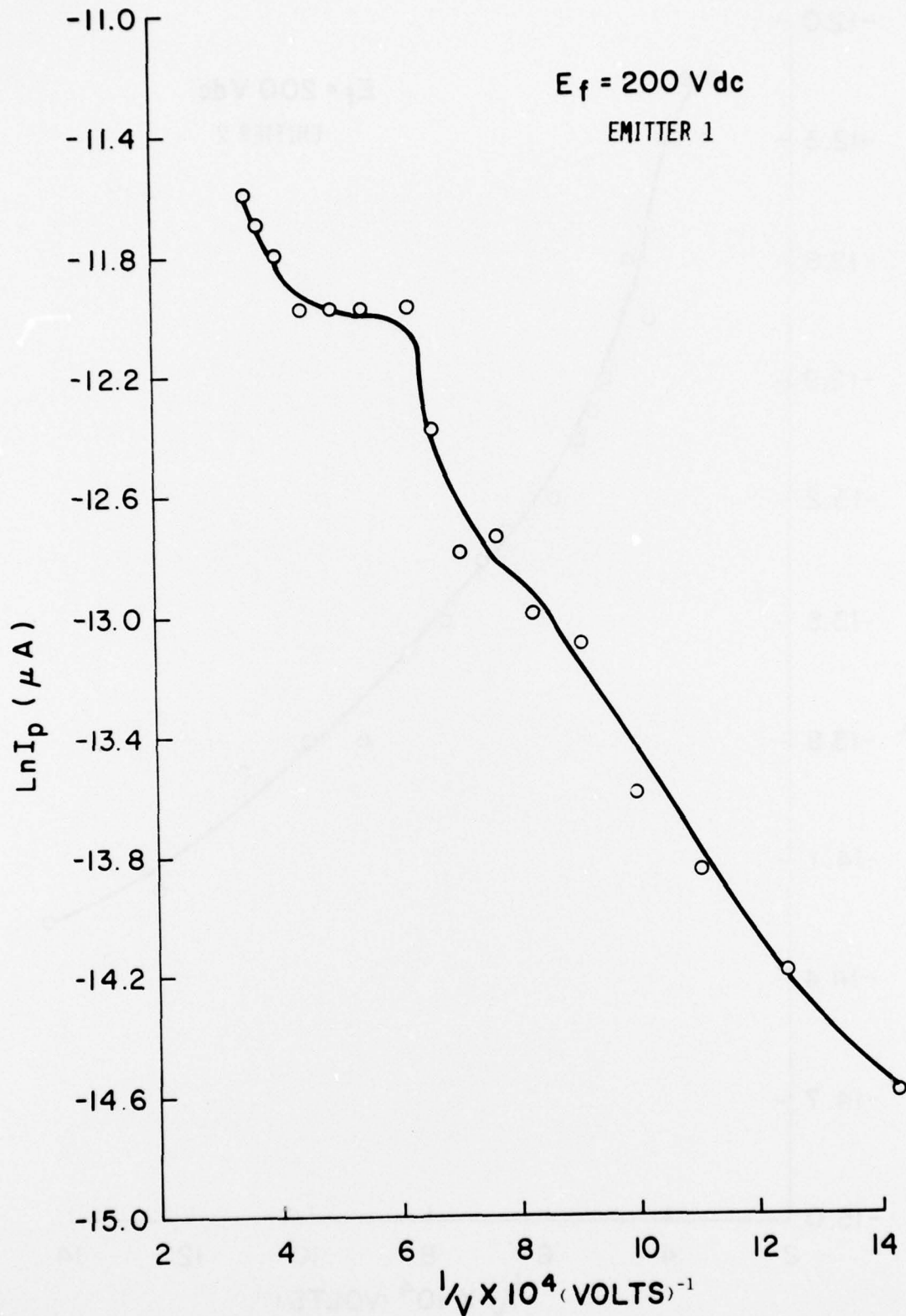


FIG. 15 MODIFIED FIELD PLOT OF  $\text{SnO}_2$  COLD CATHODE (EMITTER 1)

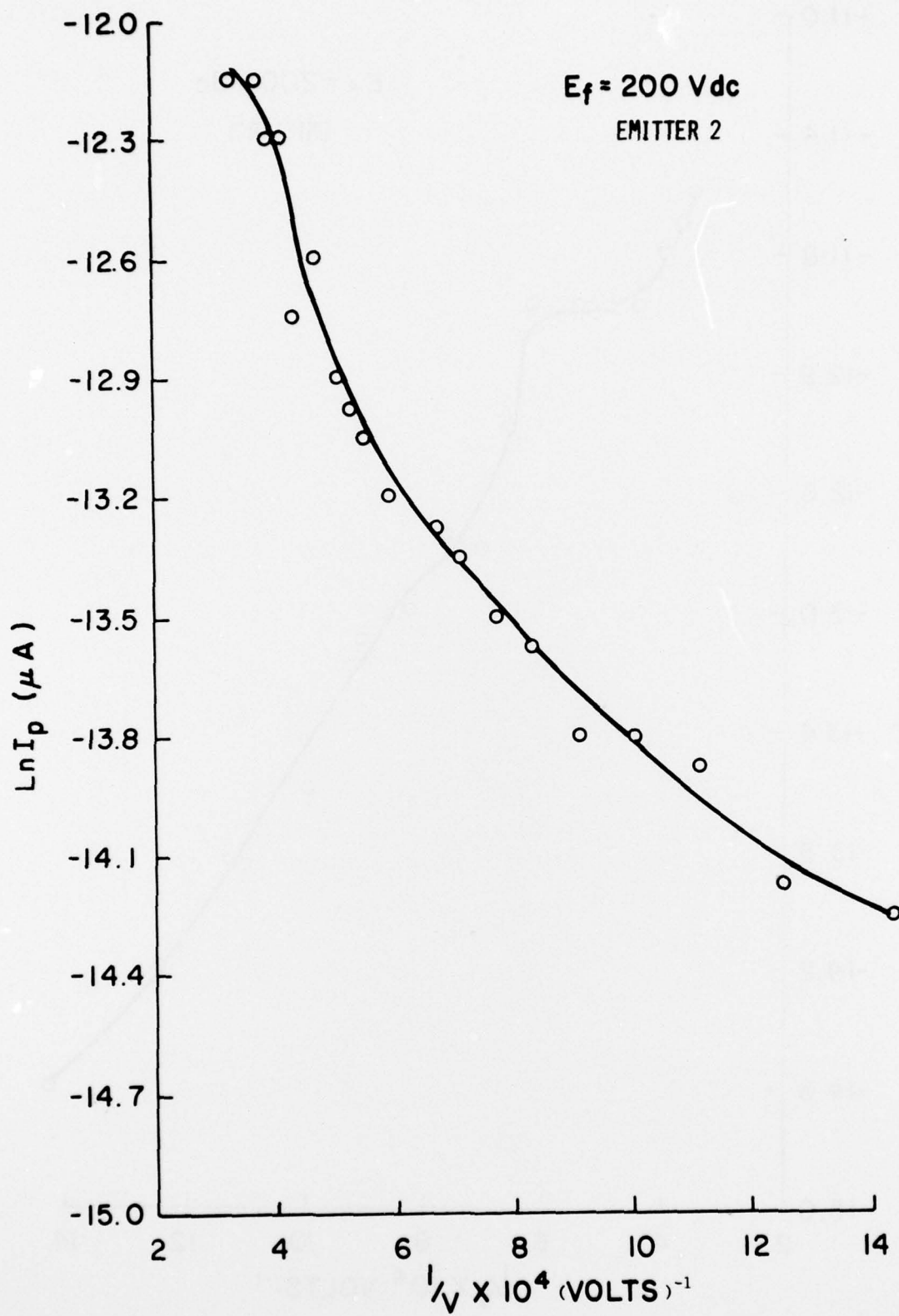


FIG. 16 MODIFIED FIELD PLOT OF  $\text{SnO}_2$  COLD CATHODE (EMITTER 2)

TABLE 1  
 SIGNIFICANT OPERATING CHARACTERISTICS OF A REPRESENTATIVE CROSS-SECTION OF THE VARIOUS  
 EMITTERS STUDIED

ARRAY NO.	DOPING ATOMS/ cm <sup>3</sup>	FILM THICKNESS (MICRONS)	NO. OF ELEMENTS	FILM VOLTAGE (Volts, dc)	% EFFICIENCY $\left( \frac{I_p}{I_f} \times 100 \right)$	FILM CURRENT (mA, dc)	COLLECTOR CURRENT (μA, dc)
1	—	0.10 μ	10	160 170 180 200	3.7 5.7 3.5 6.3	0.3 0.5 0.4 0.3	11 27 15 17
2	$2 \times 10^{21}$	0.10 μ	5	110 130 150 180	1.1 1.0 0.6 0.9	4.1 4.2 6.3 5.5	46 41 41 49
3	$2 \times 10^{22}$	0.10 μ	5	75 100 120 140 160 170 180	0.2 0.2 0.1 0.1 0.1 0.1 0.1	1.5 1.5 8.6 25 81 99 100	2.3 2.7 9.5 31 90 120 145
4	$1 \times 10^{16}$	0.10 μ	5	150 175 200 225 250	6.4 3.7 7.6 2.3 0.9	0.1 0.2 0.3 0.8 1.5	3.2 7.0 26 10 14
5	$5 \times 10^{18}$	0.12 μ	5	60 ELEMENTS INTERDIGITATED 75 85 90 95 100 110 120 130 135 140 150 160	0.1 0.1 0.1 0.1 0.2 0.5 0.8 0.9 1.0 0.9 1.0 1.0 1.0	100 82 79 70 75 61 51 45 53 45 43 39 33	48 75 90 90 100 132 248 370 500 430 385 405 330
6	—	0.10 μ	5	ELEMENTS INTERDIGITATED 150 170 190 210 230 250	0.1 0.2 0.9 1.8 2.0 3.8	13 17 26 23 22 15	12 36 240 420 450 570

TABLE 1 (Contd)

ARRAY NO.	DOPING ATOMS/ cm <sup>3</sup>	FILM THICKNESS (MICRONS)	NO. OF ELEMENTS	FILM VOLTAGE (Volts, dc)	% EFFICIENCY $\left( \frac{I_p}{I_f} \times 100 \right)$	FILM CURRENT (mA, dc)	COLLECTOR CURRENT (μA, dc)
7	UNDOPED	0.10 μ	5	175	1.1	0.3	3.6
				200	0.2	0.4	0.9
				225	0.2	0.7	1.6
				250	3.6	1.1	40
8	$5 \times 10^{16}$	0.05 μ	1	325	0.4	6.0	25
				350	0.8	3.2	26
				375	0.7	5.9	41
				400	0.8	5.3	43
9	UNDOPED	0.10 μ	1	150	0.1	2.9	3.5
				175	0.1	3.6	3.5
				200	0.6	6.1	36
				225	0.3	6.5	22
				250	0.5	6.7	32
				275	0.4	6.5	25
				300	14	0.1	11
10	$5 \times 10^{17}$	0.05 μ	1	300	4.1	2.8	115
				325	4.8	2.9	140
				350	5.2	2.2	115
11	$5 \times 10^{18}$	0.10 μ	1	225	12	0.2	23
				250	7.7	0.3	20
				275	1.8	0.4	7.0
				300	1.8	0.4	7.0
				325	2.5	0.4	10
				350	2.1	0.8	17
				400	1.8	0.9	16
				425	1.0	1.0	10
12			1	340	16	73 (μA)	12